PROCEEDINGS OF SCIENCE

Analysis of the doubly radiative decays $\eta^{(\prime)} \to \pi^0\gamma\gamma$ and $\eta' \to \eta\gamma\gamma$

Rafel Escribano,[a,b] **Sergi Gonzàlez-Solís**[c,*] **and Emilio Royo**[a,b]

[a] *Grup de Física Teòrica, Departament de Física, Universitat Autònoma de Barcelona, 08193 Bellaterra (Barcelona), Spain*

[b] *Institut de Física d'Altes Energies (IFAE) and The Barcelona Institute of Science and Technology, Campus UAB, 08193 Bellaterra (Barcelona), Spain*

[c] *Theoretical Division, Los Alamos National Laboratory, Los Alamos, NM 87545, USA*

E-mail: sergig@lanl.gov

We study the doubly radiative decays $\eta^{(\prime)} \to \pi^0\gamma\gamma$ and $\eta' \to \eta\gamma\gamma$ in terms of vector and scalar meson exchange contributions using, respectively, the frameworks of Vector Meson Dominance and the Linear Sigma model. Predictions for the $m^2_{\gamma\gamma}$ invariant mass distribution and branching ratios are given, and a discussion of how they compare to experimental data is carried out.

Preprint number: LA-UR-22-22732

The 10th International Workshop on Chiral Dynamics - CD2021
15-19 November 2021
Online

*Speaker

PoS(CD2021)028

1. Introduction

In this contribution, we study the rare, doubly radiative decay $\eta \to \pi^0\gamma\gamma$, as well as the partner reactions $\eta' \to \pi^0\gamma\gamma$ and $\eta' \to \eta\gamma\gamma$. The reason to study the decay $\eta \to \pi^0\gamma\gamma$ is manifold. On the one hand, this process has attracted the attention of the Chiral Perturbation Theory community over the years as this reaction is an excellent laboratory to test the predictive power of this theory. In detail, the resulting tree-level calculations at $O(p^2)$ and $O(p^4)$ vanish because in the chiral Lagrangian there is no direct coupling of photons to the neutral π^0 and η mesons [1]. The first non-zero contribution comes from $O(p^4)$ charged pion and kaon loops, but these are greatly suppressed because they violate G-parity in the vertex $\eta\pi^0\pi^+\pi^-$, in the case of the former, and due to the smallness of the loop integration in the latter case. The first sizable contribution comes at $O(p^6)$, but the associated low-energy constants are not well defined and one must resort to phenomenological models, such as vector meson dominance (VMD) [1–3] or the Nambu-Jona-Lasinio model [4–6], to determine them. However, since vector mesons are essential for the description of this process, their dynamical role has to be included systematically with the full vector meson propagator [1, 7–10]. Fig 1 shows a visual summary of the current status of the decay width including most recent experimental measurements and theoretical predictions. As it can be observed, despite both experimental and theoretical efforts, the situation is not conclusive yet and new and more precise experimental data is highly desirable, which can come, *e.g.* from KLOE-2 [11] or from the new Jefferson Lab Eta Factory (JEF) experiment [12].

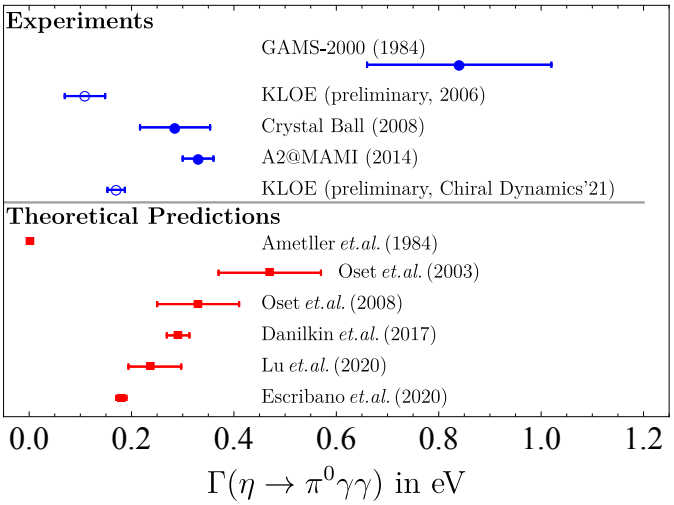

Figure 1: Status of most recent experimental measurements of the decay width $\Gamma(\eta \to \pi^0\gamma\gamma)$ (upper panel), including the results from the collaborations GAMS-2000 [15], KLOE (2006 preliminary) [16], Crystall Ball [17], A2 [18] and KLOE (preliminary, 2021) [19], compared to theoretical predictions of Ametller *et.al.* [1], Oset *et.al.* [9, 10], Lu *et.al.* [21], Danilkin *et.al.* [20] and Escribano *et.al.* [22].

Likewise, the study of the decays $\eta' \to \pi^0\gamma\gamma$ and $\eta' \to \eta\gamma\gamma$ is interesting for a number of reasons: *i*) they complete existing calculations of the partner reaction $\eta \to \pi^0\gamma\gamma$; *ii*) the BESIII collaboration has recently reported the first measurements of these decays [13, 14], thus making the topic of timely interest; *iii*) their analysis could help extract information on the properties of the lowest-lying scalar resonances, *i.e.* the $a_0(980)$ and the $\sigma(500)$ and $f_0(980)$.

The aim of this contribution is to highlight the results for the three doubly radiative decays $\eta^{(\prime)} \to \pi^0\gamma\gamma$ and $\eta' \to \eta\gamma\gamma$ obtained in [22], and it is structured as follows. The theoretical framework is detailed in Secs. 2 and 3, where the VMD and LσM calculations are described. Our results, and a discussion of how they compare to experimental data, are presented in Sec. 4. We close with a brief summary in Sec. 5.

2. Vector meson exchange contributions

To calculate the vector meson exchange contributions we use Vector Meson Dominance. The corresponding VMD amplitude represents not only the dominant contribution to the process $\eta \to \pi^0\gamma\gamma$, as shown long ago in [1], but also to the decays $\eta' \to \pi^0\gamma\gamma$ and $\eta' \to \eta\gamma\gamma$, as we will see in this contribution [22].

In the VMD framework, the $\eta \to \pi^0\gamma\gamma$ proceeds through the transition $\eta \to V\gamma$ followed by $V \to \pi^0\gamma$, resulting in a total of six diagrams contributing to the amplitude of the process, which correspond to the exchange of the three neutral vector mesons $V = \rho^0, \omega$ and ϕ in the t and u channels. The single necessary interaction terms to describe the $VP\gamma$ vertex, consistent with Lorentz, P, C and gauge invariance, can be deduced from the effective Lagrangian [23, 24]:

$$\mathcal{L}_{VP\gamma} = g\epsilon_{\mu\nu\alpha\beta}\partial^\mu A^\nu \mathrm{Tr}\left[Q\left(\partial^\alpha V^\beta P + P\partial^\alpha V^\beta\right)\right], \tag{1}$$

where g is a generic electromagnetic coupling constant, $\epsilon_{\mu\nu\alpha\beta}$ is the totally antisymmetric Levi-Civita tensor, A^μ is the photon field, V^μ and P are, respectively, the matrices for the vector and pseudoscalar meson fields, and $Q = \mathrm{diag}\{2/3, -1/3, -1/3\}$ is the quark-charge matrix. Combining the $V\eta\gamma$ and $V\pi^0\gamma$ interacting terms from Eq. (1) with the propagator of the corresponding vector meson, we can calculate the vector meson contributions to $\eta \to \pi^0\gamma\gamma$. We find the following expression for the invariant amplitude [22]:

$$\mathcal{A}^{\mathrm{VMD}}_{\eta\to\pi^0\gamma\gamma} = \sum_{V=\rho^0,\omega,\phi} g_{V\eta\gamma}g_{V\pi^0\gamma}\left[\frac{(P\cdot q_2 - m_\eta^2)\{a\} - \{b\}}{D_V(t)} + \left\{\begin{array}{c} q_2 \leftrightarrow q_1 \\ t \leftrightarrow u \end{array}\right\}\right], \tag{2}$$

where $t, u = (P - q_{2,1})^2 = m_\eta^2 - 2P\cdot q_{2,1}$ are the Mandelstam variables, $\{a\}$ and $\{b\}$ are the Lorentz structures, which are defined as

$$\begin{aligned} \{a\} &= (\epsilon_1\cdot\epsilon_2)(q_1\cdot q_2) - (\epsilon_1\cdot q_2)(\epsilon_2\cdot q_1), \\ \{b\} &= (\epsilon_1\cdot q_2)(\epsilon_2\cdot P)(P\cdot q_1) + (\epsilon_2\cdot q_1)(\epsilon_1\cdot P)(P\cdot q_2) \\ &\quad - (\epsilon_1\cdot\epsilon_2)(P\cdot q_1)(P\cdot q_2) - (\epsilon_1\cdot P)(\epsilon_2\cdot P)(q_1\cdot q_2), \end{aligned} \tag{3}$$

where P is the four-momentum of the decaying η meson, and $\epsilon_{1,2}$ and $q_{1,2}$ are, respectively, the polarisation and four-momentum vectors of the final photons. The denominator $D_V(t) = m_V^2 - t - i\, m_V\Gamma_V$ is the vector meson propagator; for the ρ^0 propagator, we use an energy-dependent decay width

$$\Gamma_{\rho^0}(t) = \Gamma_{\rho^0} \times [(t - 4m_\pi^2)/(m_{\rho^0}^2 - 4m_\pi^2)]^{3/2} \times \theta(t - 4m_\pi^2). \tag{4}$$

The amplitudes for the partner reactions $\eta' \to \pi^0\gamma\gamma$ and $\eta' \to \eta\gamma\gamma$ have a similar structure to that of Eq. (2), with the replacements $m_\eta^2 \to m_{\eta'}^2$, and $g_{V\eta\gamma}g_{V\pi^0\gamma} \to g_{V\eta'\gamma}g_{V\pi^0\gamma}$ for the $\eta' \to \pi^0\gamma\gamma$ and $g_{V\eta\gamma}g_{V\pi^0\gamma} \to g_{V\eta'\gamma}g_{V\eta\gamma}$ for the $\eta' \to \eta\gamma\gamma$.

The theoretical parametrization of the $VP\gamma$ couplings in Eq. (2), $g_{VP\gamma}$, can be written as [25, 26]:

$$\begin{aligned}
g_{\rho^0\pi^0\gamma} &= \frac{1}{3}g\,,\ g_{\rho^0\eta\gamma} = g z_{\rm NS}\cos\varphi_P\,,\ g_{\rho^0\eta'\gamma} = g z_{\rm NS}\sin\varphi_P\,,\\
g_{\omega\pi^0\gamma} &= g\cos\varphi_V\,,\\
g_{\omega\eta\gamma} &= \frac{1}{3}g\left(z_{\rm NS}\cos\varphi_P\cos\varphi_V - 2\frac{\overline{m}}{m_s}z_{\rm S}\sin\varphi_P\sin\varphi_V\right),\\
g_{\omega\eta'\gamma} &= \frac{1}{3}g\left(z_{\rm NS}\sin\varphi_P\cos\varphi_V + 2\frac{\overline{m}}{m_s}z_{\rm S}\cos\varphi_P\sin\varphi_V\right),\\
g_{\phi\pi^0\gamma} &= g\sin\varphi_V\,,\\
g_{\phi\eta\gamma} &= \frac{1}{3}g\left(z_{\rm NS}\cos\varphi_P\sin\varphi_V + 2\frac{\overline{m}}{m_s}z_{\rm S}\sin\varphi_P\cos\varphi_V\right),\\
g_{\phi\eta'\gamma} &= \frac{1}{3}g\left(z_{\rm NS}\sin\varphi_P\sin\varphi_V - 2\frac{\overline{m}}{m_s}z_{\rm S}\cos\varphi_P\cos\varphi_V\right),
\end{aligned} \tag{5}$$

where φ_P is the pseudoscalar η-η' mixing angle in the quark-flavor basis, φ_V is the vector ω-ϕ mixing angle in the same basis, $\overline{m}/m_s$ is the quotient of constituent quark masses[1], and $z_{\rm NS}$ and $z_{\rm S}$ are the *non-strange* and *strange* multiplicative factors accounting for the relative meson wavefunction overlaps [25, 26].

3. Scalar meson exchange contributions

The scalar meson exchange contributions can be obtained using the LσM. We use the complementarity between this model and ChPT to include the scalar meson poles at the same time as keeping the correct low-energy behavior expected from chiral symmetry [27].

Within this framework, the two $\eta^{(\prime)} \to \pi^0\gamma\gamma$ processes proceed through kaon loops and by exchanging the $a_0(980)$ in the s-channel and the κ in the t- and u-channels. The $\eta' \to \eta\gamma\gamma$ decay is more complex, as it proceeds through both kaon and pion loops, with the $\sigma(600)$ and the $f_0(980)$ exchanged in the s-channel for both types of loops, while in the u- and t-channels, the κ is exchanged for kaon loops and the $a_0(980)$ for pion loops. The loop contributions take place through combinations of three diagrams for each one of the intermediate states, which added together give finite results. In all, the amplitudes for the three processes in the LσM can be expressed as follows

$$\mathcal{A}^{\rm L\sigma M}_{\eta\to\pi^0\gamma\gamma} = \frac{2\alpha}{\pi}\frac{1}{m^2_{K^+}}L(s_K)\{a\}\times\mathcal{A}^{\rm L\sigma M}_{K^+K^-\to\pi^0\eta}\,, \tag{6}$$

$$\mathcal{A}^{\rm L\sigma M}_{\eta'\to\pi^0\gamma\gamma} = \frac{2\alpha}{\pi}\frac{1}{m^2_{K^+}}L(s_K)\{a\}\times\mathcal{A}^{\rm L\sigma M}_{K^+K^-\to\pi^0\eta'}\,, \tag{7}$$

$$\mathcal{A}^{\rm L\sigma M}_{\eta'\to\eta\gamma\gamma} = \frac{2\alpha}{\pi}\frac{1}{m^2_{\pi}}L(s_\pi)\{a\}\times\mathcal{A}^{\rm L\sigma M}_{\pi^+\pi^-\to\eta\eta'} + \frac{2\alpha}{\pi}\frac{1}{m^2_{K^+}}L(s_K)\{a\}\times\mathcal{A}^{\rm L\sigma M}_{K^+K^-\to\eta\eta'}\,, \tag{8}$$

[1]The flavour symmetry-breaking mechanism associated to differences in the effective magnetic moments of light (*i.e.* up and down) and strange quarks in magnetic dipolar transitions is implemented via constituent quark mass differences. Specifically, one introduces a multiplicative $SU(3)$-breaking term, *i.e.* $1 - s_e \equiv \overline{m}/m_s$, in the s-quark entry of the quark-charge matrix Q.

where α is the fine-structure constant, $L(z)$ is the loop integral [22], $s_{\pi,K} = s/m^2_{\pi,K}$, with s being the invariant mass of the two photons, $\{a\}$ is the Lorentz structure defined in Eq. (4), and, finally, $\mathcal{A}^{\mathrm{L}\sigma\mathrm{M}}_{\eta^{(\prime)}\pi^0\to K^+K^-}$ and $\mathcal{A}^{\mathrm{L}\sigma\mathrm{M}}_{\eta'\eta\to K^+K^-(\pi^+\pi^-)}$ are the four-pseudoscalar amplitude, whose explicit expressions can be found in [22].

4. Results

With the theoretical expression presented in Secs. 2 and 3, we are now in a position to present our results. These are obtained using the standard formula for three-body decays [28], with the absolute value of the amplitude squared given by

$$|\mathcal{A}|^2 = |\mathcal{A}^{\mathrm{VMD}}|^2 + |\mathcal{A}^{\mathrm{L}\sigma\mathrm{M}}|^2 + 2\mathrm{Re}\left[\mathcal{A}^{*\mathrm{VMD}}\mathcal{A}^{\mathrm{L}\sigma\mathrm{M}}\right], \tag{9}$$

where $\mathcal{A}^{\mathrm{VMD}}$ and $\mathcal{A}^{\mathrm{L}\sigma\mathrm{M}}$ contain the vector and scalar resonance exchange contributions as defined in the previous sections. The last term in Eq. (9) represents the interference between the vector and scalar effects.

For our analysis, we use the masses and decay widths of the participating resonances from the PDG [28], and employ $f_\pi = 92.07$ MeV and $f_K = 110.10$ MeV, for the pion and kaon decay constants, respectively. Concerning the VMD couplings, $g_{VP\gamma}$, we consider two different approaches to fix them. On the one hand, we obtain them directly from the measured $V \to P\gamma$ and $P \to V\gamma$ decay widths [28]. Using

$$\Gamma_{V\to P\gamma} = \frac{1}{3}\frac{g^2_{VP\gamma}}{32\pi}\left(\frac{m_V^2 - m_P^2}{m_V}\right)^3, \quad \Gamma_{P\to V\gamma} = \frac{g^2_{VP\gamma}}{32\pi}\left(\frac{m_P^2 - m_V^2}{m_P}\right)^3, \tag{10}$$

we obtain the values collected in Table 1.

On the other hand, we employ the expressions of the VMD couplings given in Eq. (5). For the participating parameters, we use:

$$\begin{aligned} g &= 0.70 \pm 0.01\ \mathrm{GeV}^{-1}, \quad z_S\overline{m}/m_s = 0.65 \pm 0.01, \\ \phi_P &= (41.4 \pm 0.5)^\circ, \qquad \phi_V = (3.3 \pm 0.1)^\circ, \\ z_{\mathrm{NS}} &= 0.83 \pm 0.02, \end{aligned} \tag{11}$$

Decay	BR [28]	$\lvert g_{VP\gamma}\rvert$ GeV^{-1}
$\rho^0 \to \pi^0\gamma$	$(4.7 \pm 0.6) \times 10^{-4}$	0.22(1)
$\rho^0 \to \eta\gamma$	$(3.00 \pm 0.21) \times 10^{-4}$	0.48(2)
$\eta' \to \rho^0\gamma$	$(28.9 \pm 0.5)\%$	0.40(1)
$\omega \to \pi^0\gamma$	$(8.40 \pm 0.22)\%$	0.70(1)
$\omega \to \eta\gamma$	$(4.5 \pm 0.4) \times 10^{-4}$	0.135(6)
$\eta' \to \omega\gamma$	$(2.62 \pm 0.13)\%$	0.127(4)
$\phi \to \pi^0\gamma$	$(1.30 \pm 0.05) \times 10^{-3}$	0.041(1)
$\phi \to \eta\gamma$	$(1.303 \pm 0.025)\%$	0.2093(20)
$\phi \to \eta'\gamma$	$(6.22 \pm 0.21) \times 10^{-5}$	0.216(4)

Table 1: PDG values for the branching ratios of the $V(P) \to P(V)\gamma$ transitions and the calculated $g_{VP\gamma}$ couplings directly from experiment (cf. Eq. (10)).

Decay	Couplings	LσM	VMD	Γ_{th}	BR_{th}	BR_{exp} [28]
$\eta \to \pi^0\gamma\gamma$ (eV)	Empirical	5.0×10^{-4}	0.16(1)	0.18(1)	$1.35(8) \times 10^{-4}$	$2.56(22) \times 10^{-4}$
	Model-based	5.0×10^{-4}	0.16(1)	0.17(1)	$1.30(1) \times 10^{-4}$	
$\eta' \to \pi^0\gamma\gamma$ (keV)	Empirical	1.3×10^{-4}	0.57(3)	0.57(3)	$2.91(21) \times 10^{-3}$	$3.20(7)(23) \times 10^{-3}$
	Model-based	1.3×10^{-4}	0.70(4)	0.70(4)	$3.57(25) \times 10^{-3}$	
$\eta' \to \eta\gamma\gamma$ (eV)	Empirical	3.29	21.2(1.2)	23.0(1.2)	$1.17(8) \times 10^{-4}$	$8.25(3.41)(0.72) \times 10^{-5}$
	Model-based	3.29	19.1(1.0)	20.9(1.0)	$1.07(7) \times 10^{-4}$	

Table 2: Chiral-loop, LσM and VMD predictions for the $\eta \to \pi^0\gamma\gamma$, $\eta' \to \pi^0\gamma\gamma$ and $\eta' \to \eta\gamma\gamma$ decays with empirical and model-based VMD couplings. The total decay widths are calculated from the coherent sum of the LσM and VMD contributions.

which have been obtained in [26] after performing an optimization fit to the most up-to-date $VP\gamma$ experimental data. Hereafter, we refer to the former couplings as empirical and the later as model-based couplings.

In Table 2 we present our predictions for the decay widths of the three proceesses using both the empirical and model-based VMD couplings. There, we show the individual contributions from the LσM and VMD, along with the total decay width and the corresponding branching ratio (the quoted errors come from the errors associated to the $g_{VP\gamma}$ couplings), and the associated experimental value from the PDG. In Fig. 2, we show our predictions for the $\eta \to \pi^0\gamma\gamma$ (left) and $\eta' \to \pi^0\gamma\gamma$ (right) diphoton invariant mass distribution compared with the experimental data, whilst in Fig. 3 we show the different contributions to the $\eta' \to \eta\gamma\gamma$ energy spectrum.

Comments on these results are in order:

- Our predictions in Table 2 for the three processes are robust against variations of the VMD couplings we have employed.
- The shape of the measured spectra of $\eta \to \pi^0\gamma\gamma$ and $\eta' \to \pi^0\gamma\gamma$ is well captured by our predictions, see Fig. 2. However, while our theoretical treatment shows a very good agreement with the $\eta' \to \pi^0\gamma\gamma$ spectra measured by BESIII [13], the exact same treatment for the spectrum of the decay $\eta \to \pi^0\gamma\gamma$ appears to present a normalization offset with respect to the experimental measurements by the A2 [18] and Crystal Ball [17] collaborations, and the branching ratio is found to be approximately half of the corresponding experimental values (see Table 2). However, it is important to note that our predictions for this channel are in good agreement with the preliminary results from KLOE presented in this workshop [19] (see also [11]).
- Our branching ratio predictions for $\eta' \to \eta\gamma\gamma$ are consistent with the BESIII experimental value [14].

5. Summary and outlook

We have presented a theoretical analysis of the doubly radiative decays $\eta^{(\prime)} \to \pi^0\gamma\gamma$ and $\eta' \to \eta\gamma\gamma$ using the VMD and LσM frameworks to account for the vector and scalar meson resonance exchange contributions, respectively. Our results depend on the participant VMD coupling

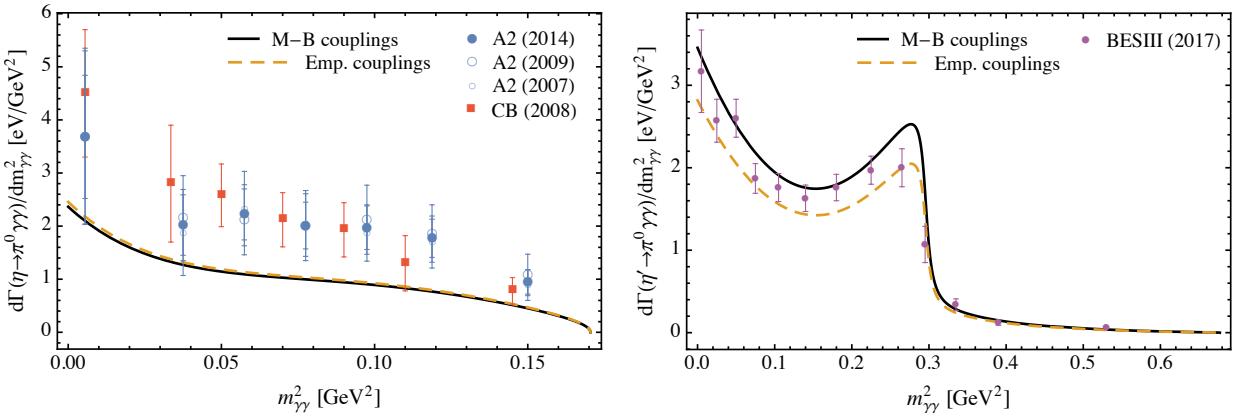

Figure 2: Comparison between the experimental diphoton energy spectra for the $\eta \to \pi^0\gamma\gamma$ and $\eta' \to \pi^0\gamma\gamma$ and our theoretical predictions using the empirical and model-based VMD couplings. The experimental data is taken from Ref. [18] (A2), Ref. [17] (Crystal Ball) and Ref. [13] (BESIII).

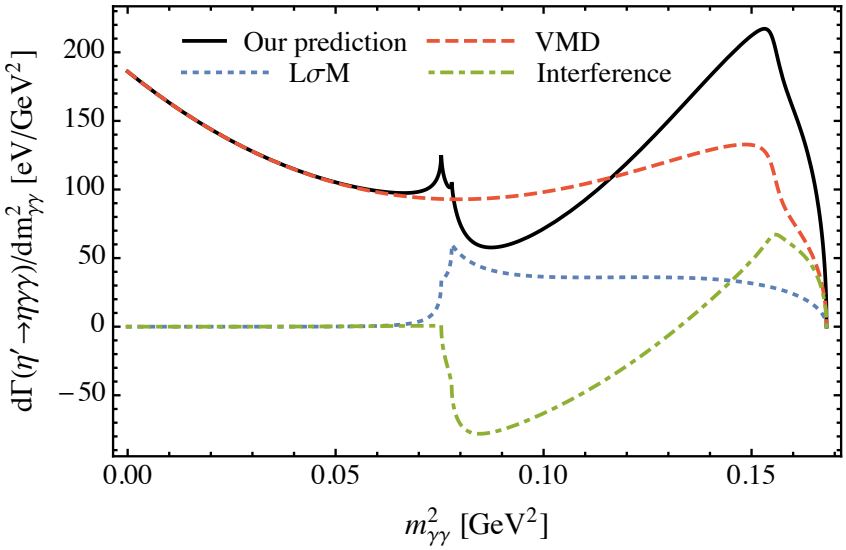

Figure 3: Contributions to the $\eta' \to \eta\gamma\gamma$ diphoton energy spectrum (solid black), using the model-based VMD couplings, from intermediate vector (dashed magenta) and scalar (dashed brown) meson exchanges, and their interference (dot-dashed cyan).

constants, $g_{VP\gamma}$, which we fix following two different paths: directly from the experimental decay $V(P) \to P(V)\gamma$ decay widths (see Table 1) or from a phenomenological quark-based model supplemented by a fit to experimental data (see Eqs. (5) and (11)). We refer to the former couplings as empirical and the later as model-based couplings. Our results for the decay widths and branching ratios are summarized in Table 2, while our predictions for the invariant mass distribution are show in Figs. 2 and 3, and a discussion of the results obtained and how they compare to available experimental data has been carried out at the end of section 4. As a final remark, these decays provide a good environment to search for GeV-signatures of a leptophobic B boson [29, 30].

References

[1] L. Ametller, J. Bijnens, A. Bramon and F. Cornet, Phys. Lett. B **276**, 185 (1992).

[2] P. Ko, Phys. Lett. B **349** (1995), 555-560 [arXiv:hep-ph/9503253 [hep-ph]].

[3] M. Jetter, Nucl. Phys. B **459** (1996), 283-310 [arXiv:hep-ph/9508407 [hep-ph]].

[4] A. A. Bel'kov, A. V. Lanyov and S. Scherer, J. Phys. G **22** (1996), 1383-1394 [arXiv:hep-ph/9506406 [hep-ph]].

[5] S. Bellucci and C. Bruno, Nucl. Phys. B **452** (1995), 626-648 [arXiv:hep-ph/9502243 [hep-ph]].

[6] J. Bijnens, A. Fayyazuddin and J. Prades, Phys. Lett. B **379** (1996), 209-218 [arXiv:hep-ph/9512374 [hep-ph]].

[7] C. Picciotto, Nuovo Cim. A **105**, 27 (1992).

[8] J. N. Ng and D. J. Peters, Phys. Rev. D **46**, 5034 (1992).

[9] E. Oset, J. R. Pelaez and L. Roca, Phys. Rev. D **67**, 073013 (2003) [hep-ph/0210282].

[10] E. Oset, J. R. Pelaez and L. Roca, Phys. Rev. D **77**, 073001 (2008) [arXiv:0801.2633 [hep-ph]].

[11] B. Cao [KLOE-2], PoS **EPS-HEP2021** (2022), 409

[12] L. Gan *et.al.*, Update to the JEF proposal (PR12-14-004), https://www.jlab.org/exp_prog/proposals/17/C12-14-004.pdf

[13] M. Ablikim *et al.* [BESIII Collaboration], Phys. Rev. D **96**, no. 1, 012005 (2017) [arXiv:1612.05721 [hep-ex]].

[14] M. Ablikim *et al.* [BESIII Collaboration], Phys. Rev. D **100**, no. 5, 052015 (2019) [arXiv:1906.10346 [hep-ex]].

[15] D. Alde *et al.* [Serpukhov-Brussels-Annecy(LAPP) and Soviet-CERN Collaborations], Z. Phys. C **25**, 225 (1984) [Yad. Fiz. **40**, 1447 (1984)].

[16] B. Di Micco *et al.* [KLOE Collaboration], Acta Phys. Slov. **56**, 403 (2006).

[17] S. Prakhov, B. M. K. Nefkens, C. E. Allgower, V. Bekrenev, W. J. Briscoe, J. R. Comfort, K. Craig and D. Grosnick *et al.*, Phys. Rev. C **78**, 015206 (2008).

[18] B. M. K. Nefkens *et al.* [A2 at MAMI Collaboration], Phys. Rev. C **90**, no. 2, 025206 (2014) [arXiv:1405.4904 [hep-ex]].

[19] E. P. del Rio, Hadron physics results at KLOE-2 experiment, https://indico.ihep.ac.cn/event/14770/session/1/contribution/198/material/slides/0.pdf

[20] I. Danilkin, O. Deineka and M. Vanderhaeghen, Phys. Rev. D **96**, no. 11, 114018 (2017) [arXiv:1709.08595 [hep-ph]].

[21] J. Lu and B. Moussallam, Eur. Phys. J. C **80** (2020) no.5, 436 [arXiv:2002.04441 [hep-ph]].

[22] R. Escribano, S. Gonzàlez-Solís, R. Jora and E. Royo, Phys. Rev. D **102** (2020) no.3, 034026 [arXiv:1812.08454 [hep-ph]].

[23] A. Bramon, R. Escribano and M. D. Scadron, Eur. Phys. J. C **7** (1999), 271-278 [arXiv:hep-ph/9711229 [hep-ph]].

[24] T. P. Cheng, Phys. Rev. **162** (1967), 1734-1738

[25] A. Bramon, R. Escribano and M. Scadron, Phys. Lett. B **503** (2001), 271-276 [arXiv:hep-ph/0012049 [hep-ph]].

[26] R. Escribano and E. Royo, Phys. Lett. B **807** (2020), 135534 [arXiv:2003.08379 [hep-ph]].

[27] R. Escribano, Phys. Rev. D **74**, 114020 (2006) [hep-ph/0606314].

[28] P.A. Zyla *et al.* [Particle Data Group], PTEP **2020** (2020) no.8, 083C01

[29] J. Elam *et al.* [REDTOP], [arXiv:2203.07651 [hep-ex]].

[30] R. Escribano, S. Gonzàlez-Solís and E. Royo, in preparation.